ISTITUTO DI ANALISI DEI SISTEMI ED INFORMATICA
CONSIGLIO NAZIONALE DELLE RICERCHE

A. Bertuzzi, A. Fasano, L. Filidoro, A. Gandolfi, C. Sinisgalli

DYNAMICS OF TUMOUR CORDS FOLLOWING CHANGES IN OXYGEN AVAILABILITY: A MODEL INCLUDING A DELAYED EXIT FROM QUIESCENCE

R. 593 Luglio 2003

Alessandro Bertuzzi – Istituto di Analisi dei Sistemi ed Informatica del CNR, viale Manzoni 30 - 00185 Roma, Italy. Email : bertuzzi@iasi.cnr.it.

Antonio Fasano – Dipartimento di Matematica "U. Dini", Università di Firenze, viale Morgagni 67/A - 50134 Firenze, Italy. Email : fasano@math.unifi.it.

Lucianna Filidoro – Istituto di Analisi dei Sistemi ed Informatica del CNR, viale Manzoni 30 - 00185 Roma, Italy. Email : lfilidor@ikra.med.uni-muenchen.de.

Alberto Gandolfi – Istituto di Analisi dei Sistemi ed Informatica del CNR, viale Manzoni 30 - 00185 Roma, Italy. Email : gandolfi@iasi.cnr.it.

Carmela Sinisgalli – Istituto di Analisi dei Sistemi ed Informatica del CNR, viale Manzoni 30 - 00185 Roma, Italy. Email : sinisgalli@iasi.cnr.it.

This work was partially supported by CIMAB, Italy, by the Progetto Strategico CNR "Metodi e Modelli Matematici nello Studio dei Fenomeni Biologici", and by the National Research Project "Problemi a Frontiera Libera", co-financed by MIUR.

ISSN: 1128–3378

Collana dei Rapporti
dell'Istituto di Analisi dei Sistemi ed Informatica, CNR

viale Manzoni 30, 00185 ROMA, Italy

tel. ++39-06-77161
fax ++39-06-7716461
email: iasi@iasi.rm.cnr.it
URL: http://www.iasi.rm.cnr.it

Abstract

Abstract. In this paper we investigate the formation of tumour cords (cylindrical arrangements of tumour cells around blood vessels) within a tumour tissue. The shrinkage and the expansion of the cord following a stepwise decrease or, respectively, increase of oxygen tension in the blood vessel are also described. The model represents the tumour cell population as a continuum and includes two novel aspects with respect to our previous works: cell death does not occur instantaneously, but is preceded by a reversible pre-necrotic state; the recruitment of cells from quiescence into proliferation may require a recovery period. Model predictions are compared with experimental data reported by Hirst *et al.* (1991).

Key words: Tumour cords, oxygen diffusion, continuum modelling, free boundary problems.

1. Introduction

In some experimental and human tumours, it is possible to observe cylindrical arrangements of tumour cells around blood vessels. Such structures have been named *tumour cords* [1,2,3,4]. The cords are in general surrounded by regions of necrosis, since the oxygen tension and the concentration of nutrients such as glucose decay radially within the cord and, when they fall below some critical values, cell death occurs. When necrosis is present, the mean thickness of the cords (*i.e.*, the distance between the vessel wall and the first layer of necrotic cells) has been found to be 60–130 μm in different tumours, whereas the mean radius of the central vessel is in the range 10–40 μm. As a consequence of cell proliferation within the cord, outward directed cell migration occurs. The proliferation appears to slow down from the vessel wall to the periphery of the cord, and this reduction in proliferative activity is likely to be related to the decrease of the concentration of oxygen, nutrients, and/or other critical chemicals. Recently, mathematical models have been proposed to describe the stationary state of the cord [5,6,7,8] and the formation of a single cord within a normal tissue [9,10]. A model for the response of tumour cords to a single dose of radiation or anticancer drug has been proposed in [11,12].

Among the various factors that influence the proliferative activity and that are necessary for cell viability, oxygen concentration plays a major role, and experimental observations have shown the marked effect of oxygen concentration in blood on the radius of tumour cords [13,14]. In the present paper we investigate the process of cord formation within a tumour tissue, which is initially well oxygenated with vessels having a constant blood oxygen tension. This process leads to isolated cords surrounded by necrosis (section 2). Moreover, the shrinkage and the expansion of the cord following the sudden decrease or, respectively, increase of blood oxygen tension, are described (sections 3, 4 and 5). The present formulation of the model includes two novel aspects with respect to our previous works: cell death does not occur instantaneously, but is preceded by a reversible pre-necrotic state [13]; the recruitment of cells from quiescence into proliferation may require a recovery period [15,16], due to the need of re-synthesizing some proteins that are degraded during quiescence (see section 5). A comparison with the experimental data reported by Hirst *et al.* (1991) [13] is also presented (section 6).

2. Formation of the tumour cord

We start by developing a model that describes the formation of a tumour cord and of the surrounding necrosis in a vascularized tumour. In this analysis we will mainly refer to the core region of an experimental tumour implanted subcutaneously, after angiogenesis has provided in that region a suitable vascularization. So, in an ideal case, let us suppose that at an initial time, say $t=0$, the tumour tissue is well supplied with oxygen and nutrients by a regular array of parallel and identical blood vessels. In view of the symmetry, we concentrate on a vessel in the core of the array, and we fix a reference system of cylindrical coordinates on the vessel axis. Vessels are supposed to be displaced by the growth of the tumour tissue so that the intervessel distance increases (see Fig. 1). Let r be the radial distance from the axis of the vessel, and r_0 be the vessel radius.

In the framework of a continuum approach, the tumour cell population will be described by the volume fraction occupied locally by the cells. The remaining volume, which is filled by the extracellular matrix and the interstitial fluid, forms a complementary volume fraction which is supposed to be constant in space and time (assumption *(i)*). The other assumptions of the model are summarized as follows: *(ii)* Cylindrical symmetry around the reference vessel is assumed,

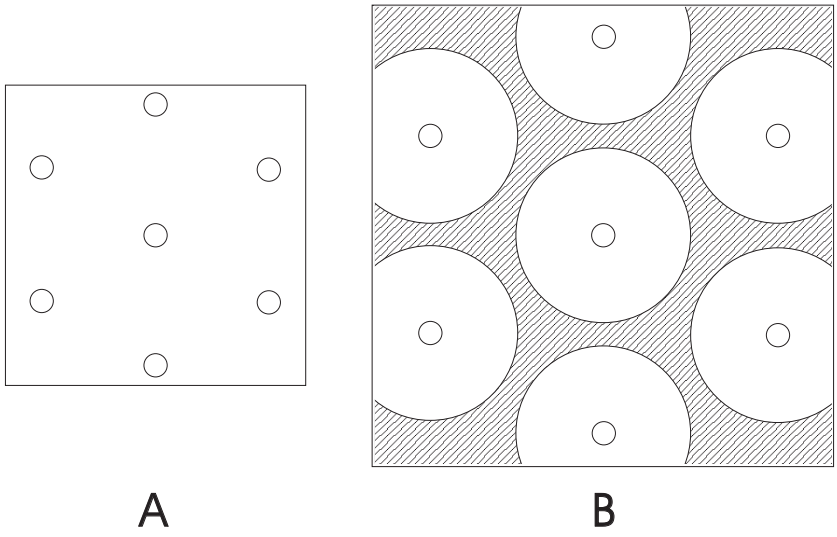

Fig. 1. Growth of vascularized tumour tissue (A) with displacement of the vessels, represented by the small circles, and formation of necrosis (hatched area) separating the cords (B).

and the cell velocity and the concentrations of chemicals are independent of the axial coordinate. *(iii)* Cell velocity is radially directed. *(iv)* Oxygen is the only species of "nutrient" considered. We denote by $\sigma(r,t)$ the local oxygen concentration, without distinguishing intracellular from extracellular concentration. *(v)* The rate of cell proliferation (*i.e.*, the rate of increment of cell volume per unit cell volume) is a nondecreasing C^1 function of σ, $\chi(\sigma)$; we assume the existence of a value σ_Q such that, below σ_Q, all cells become quiescent and $\chi(\sigma)=0$. A different hypothesis that accounts for the possibility that cells do not resume instantaneously the proliferative status from quiescence will be considered in section 5. *(vi)* If σ decreases to a threshold value σ_N ($\sigma_N<\sigma_Q$), the quiescent cells enter a pre-necrotic state in which they do not consume oxygen. After a time interval τ in this state, the cells die. Experimental obervations have shown indeed that anoxic cells can survive for a time of 6-16 h [13]. Cells in the pre-necrotic state return instantaneously to consume oxygen and their committment to death ceases if σ rises above σ_N. *(vii)* Cell death when σ is larger than σ_N is neglected. *(viii)* Dead cells are degraded to a fluid waste with a rate constant μ. Waste products are removed by the longitudinal flow of the interstitial liquid.

From the mass balance and the assumption that the volume fraction of cells (viable, pre-necrotic, and dead) is constant, the cell velocity field can be easily obtained. Denoting by $u(r,t)$ the cell velocity at distance r and time t, assumption *(i)* leads to the equation

$$\operatorname{div} u = \begin{cases} \chi(\sigma) & \text{in } P\cup Q\cup R \\ -\mu & \text{in } N\,, \end{cases} \tag{1}$$

where P denotes the region in which cell proliferation occurs, Q the region of quiescence, R the region of quiescent cells reversibly committed to death, and N the necrotic region. Concerning the concentration of oxygen, diffusion is the dominant transport mechanism and it occurs in a quasi-stationary regime. As discussed in [11], the convective transport of oxygen by interstitial

fluids can indeed be disregarded. Thus, $\sigma(r,t)$ satisfies the equation

$$\Delta\sigma = f(\sigma)\,, \tag{2}$$

where $f(\sigma)$ represents the ratio between the consumption rate in the unit volume and the diffusion coefficient. Because of assumption *(vi)*, $f(\sigma)$ must be zero for $\sigma \leq \sigma_N$, whereas we have chosen a Michaelis-Menten form for $\sigma > \sigma_N$, so we have:

$$f(\sigma) = \begin{cases} F\dfrac{\sigma}{K+\sigma} & \sigma > \sigma_N \\ 0 & \sigma \leq \sigma_N\,. \end{cases} \tag{3}$$

Finally, according to assumption *(ii)*, before the formation of the pre-necrotic region the oxygen concentration attains a minimum on a cylindrical surface at $r = B(t)$, which is also the outer boundary of the cord. Since in view of symmetry there is no mass exchange through this boundary, $B(t)$ is a material surface, so that

$$\dot{B} = u(B,t)\,. \tag{4}$$

The previously stated assumptions allow us to describe the formation of the cord as follows. For $t > 0$, and as long as $\sigma(r,t) > \sigma_N$, the evolution of the boundary B and of the concentration $\sigma(r,t)$, $r_0 \leq r \leq B(t)$, will be given by the solution of Eq. (2) with the boundary conditions

$$\sigma(r_0,t) = \sigma^\star \tag{5}$$

$$\sigma_r(B(t),t) = 0\,, \tag{6}$$

where $B(t)$, using Eq. (1) with $u(r_0,t)=0$ and (4), is expressed as

$$B(t)\dot{B}(t) = \int_{r_0}^{B(t)} r\chi(\sigma(r,t))\,dr \tag{7}$$

$$B(0) = B_0\,, \tag{8}$$

B_0 being the initial condition. B_0 has to be sufficiently close to r_0 so that the solution of Eqs. (2), (5) and (6) for $t=0$ gives $\sigma(B_0,0) > \sigma_N$. The oxygen concentration in blood, $\sigma^\star$, is taken constant in time and larger than σ_Q, so that $\chi(\sigma^\star) > 0$. We observe that $B(t)$ is increasing with time since χ is nonnegative and positive near r_0, and that the solution of Eqs. (2), (5) and (6) depends on time only through the time dependence of B.

We have:

Proposition 1. *For any constant B, $r_0 < B \leq B_N$, there exists a unique solution $\sigma(r;B)$ of Eqs. (2), (5), (6). This solution has a unique minimum at $r = B(t)$. Moreover, B_N is such that:*

$$\sigma(B_N;B_N) = \sigma_N\,, \tag{9}$$

and σ depends monotonically on B, with $\partial\sigma/\partial B$ satisfying

$$-B_N f(\sigma^\star)\log\frac{B_N}{r_0} < \frac{\partial\sigma}{\partial B} < 0\,, \quad r_0 < r \leq B\,. \tag{10}$$

Proof. Let us consider the Cauchy problem defined by Eqs. (2), (5) and

$$\sigma_r(r_0) = \Sigma^\star \,,$$

with $\Sigma^\star < 0$. We have

$$r\sigma_r(r) = r_0\Sigma^\star + \int_{r_0}^{r} r' f(\sigma(r'))\, dr' \tag{11}$$

and therefore $\sigma(r)$ is the unique solution of the following nonlinear Volterra equation

$$\sigma(r) = \sigma^\star + r_0\Sigma^\star \log\frac{r}{r_0} + \int_{r_0}^{r} r' f(\sigma(r')) \log\frac{r'}{r_0}\, dr' \,. \tag{12}$$

Obviously, for any $\Sigma^\star$, the solution σ has at most one minimum. From (12), we deduce that $\partial\sigma/\partial\Sigma^\star$ satisfies the linear Volterra equation

$$\frac{\partial\sigma}{\partial\Sigma^\star} = r_0 \log\frac{r}{r_0} + \int_{r_0}^{r} r' f'(\sigma(r'))\frac{\partial\sigma}{\partial\Sigma^\star} \log\frac{r'}{r_0}\, dr' \,,$$

implying that, for $r > r_0$,

$$\frac{\partial\sigma}{\partial\Sigma^\star} > 0 \,. \tag{13}$$

Differentiating (11) with respect to $\Sigma^\star$ we find

$$r\frac{\partial\sigma_r}{\partial\Sigma^\star} = r_0 + \int_{r_0}^{r} r' f'(\sigma(r'))\frac{\partial\sigma}{\partial\Sigma^\star}\, dr'$$

which, in view of (13), yields

$$\frac{\partial\sigma_r}{\partial\Sigma^\star} > 0 \,. \tag{14}$$

From the monotone dependence of σ and σ_r on $\Sigma^\star$ we deduce that:
(i) there exists a unique $\Sigma^\star_N < 0$ such that the corresponding function σ has the absolute minimum equal to σ_N, taken for some $r = B_N$;
(ii) for $\Sigma^\star \in (\Sigma^\star_N, 0)$ the function σ takes its minimum at a point $B(\Sigma^\star) < B_N$;
(iii) $\partial B/\partial\Sigma^\star < 0$ and $\partial\sigma(B(\Sigma^\star))/\partial\Sigma^\star > 0$. As a consequence, for any given $B \in (r_0, B_N)$, there exists one and only one $\Sigma^\star \in (\Sigma^\star_N, 0)$ such that $B(\Sigma^\star) = B$.

From (13) and $\partial B/\partial\Sigma^\star > 0$, we may infer that

$$\frac{\partial\sigma}{\partial B} < 0 \,, \quad r_0 < r \le B \,. \tag{15}$$

Recalling that the following integral equation for $\sigma(r; B)$ holds

$$\sigma(r; B) = \sigma^\star - \int_{r_0}^{B} r' f(\sigma(r'; B)) \log\frac{\min[r', r]}{r_0}\, dr' \,,$$

by direct computation we see that

$$\frac{\partial\sigma}{\partial B} = -Bf(\sigma(B; B)) \log\frac{r}{r_0} - \int_{r_0}^{B} r' f'(\sigma(r'; B))\frac{\partial\sigma}{\partial B} \log\frac{\min[r', r]}{r_0}\, dr' \,,$$

which, together with (15), provides the lower estimate

$$\frac{\partial\sigma}{\partial B} > -B_N f(\sigma^\star)\log\frac{B_N}{r_0}\,,$$

that completes the proof of property (10). ∎

The above proposition guarantees that, if instead of a constant B we have in (6) an increasing function $B(t)$ with range in $(r_0, B_N]$, a function $\sigma(r,t)$ is generated by (2), (5) and (6) as $\sigma(r,t)=\sigma(r;B(t))$, whose minimum for fixed t, $\sigma(B(t),t)$, decreases in t, tending to σ_N if $B(t)$ tends to B_N.

Proposition 2. *For $B_0\in(r_0,B_N)$, Problem (2), (5)-(8) has one unique solution (σ,B) with $B(t)$ strictly increasing, under the additional assumption*

$$\beta := \frac{B_N^2-r_0^2}{2}\log\frac{B_N}{r_0}\|f'\| < 1\,. \tag{16}$$

Moreover, the pair $(\sigma(B(t),t),B(t))$ is bound to reach the value (σ_N,B_N) at some finite time t_R.

Proof. Let us first investigate the dependence of $\sigma(r,t)$, solution of (2), (5), (6), on $B(t)$ prescribed as a non-decreasing Lipschitz continuous function with $B(0)=B_0$, and Lipschitz constant not exceeding $L_B=\chi(\sigma^\star)(B_N^2-r_0^2)/(2B_0)$, in some bounded time interval $[0,T]$, with $L_BT<B_N-B_0$. We have the following integral equation for σ

$$\sigma(r,t) = \sigma^\star - \int_{r_0}^{B(t)} r' f(\sigma(r',t))\log\frac{\min[r',r]}{r_0}\,dr'\,.$$

For a pair of functions B_1, B_2, let us consider the corresponding functions σ_1 and σ_2 extended according to $\sigma_i(r,t)=\sigma_i(B_i(t),t)$ for $B_i(t)<r\le B_N$, $i=1,2$. Setting $\delta\sigma=\sigma_1-\sigma_2$ we have the estimate

$$|\delta\sigma(r,t)| \le \int_{r_0}^{\min[B_1(t),B_2(t)]} r'\|f'\|\,|\delta\sigma(r',t)|\log\frac{\min[r',r]}{r_0}\,dr' + C\|B_1-B_2\|\,,$$

where C is a constant depending on the data. Owing to (16), the above inequality yields

$$\|\delta\sigma\| \le \frac{C}{1-\beta}\|B_1-B_2\|\,. \tag{17}$$

At this point we can set up a simple fixed point argument to prove the existence of a unique solution to (2),(5)-(8). For B given in the specified class of equi-Lipschitz functions, compute $\sigma(r,t)$ and define the mapping $B\to\tilde B$ by means of

$$\frac{d}{dt}\left(\frac{1}{2}\tilde B^2\right) = \int_{r_0}^{B(t)} r\chi(\sigma(r,t))\,dr\,, \qquad \tilde B(0)=B_0\,. \tag{18}$$

Note that $\tilde B$ belongs to the same set in which B has been chosen (and is continuously differentiable). Such a set is convex and compact in the sup-norm in $[0,T]$. For any pair (B_1,B_2), from (18) we derive the Gronwall type inequality

$$B_0\|\tilde B_1-\tilde B_2\|_t \le \frac{B_N^2-r_0^2}{2}\|\chi'\|\int_0^t\|\delta\sigma\|_\tau d\tau + B_N\|\chi\|\int_0^t\|B_1-B_2\|_\tau d\tau\,,$$

where $\|\cdot\|_\tau$ is the sup in $(0,\tau)$ (taken also with respect to r if needed). Using (17) we obtain

$$\|\tilde{B}_1 - \tilde{B}_2\| \leq KT\|B_1 - B_2\|\,,$$

which gives existence and uniqueness for T such that $KT<1$, applying Banach-Caccioppoli theorem. Existence is also guaranteed for larger time intervals by Schauder's theorem and uniqueness also follows by iteration of the same argument, resetting $t=0$ at the first hypothetic branching point of the solution.

Thus we conclude that Eqs. (2), (5)-(8) have one unique solution (σ, B) up to the time t_R at which $B(t_R)=B_N$. The fact that t_R must be finite follows from the following argument. From

$$-r\sigma_r = \int_r^{B(t)} r' f(\sigma(r',t))\,dr'$$

we deduce the lower estimate

$$\sigma_r > \gamma := -\frac{B_N^2 - r_0^2}{2r_0}\|f\|\,. \tag{19}$$

From (7) we have

$$\dot{B} \geq \frac{1}{B_N}\int_{r_0}^{B_0} r\,\chi(\sigma(r,t))\,dr\,.$$

Taking into account (19), it follows that $\sigma(r,t) > \sigma^\star + \gamma(r - r_0)$ for $r\in[r_0, B_0]$ and each t. Therefore we obtain the lower estimate

$$\dot{B} \geq \frac{1}{B_N}\int_{r_0}^{B_0} r\,\chi(\sigma^\star + \gamma(r-r_0))\,dr > 0\,,$$

providing an upper estimate of the time t_R at which $B(t_R)=B_N$ and thus $\sigma(B_N, t_R)=\sigma_N$. ∎

If B_0 is sufficiently close to r_0 so that $\sigma(B_0,0) > \sigma_Q$, arguing as in the proof above we can say that a time $t_Q < t_R$ exists at which $\sigma(B(t_Q), t_Q)=\sigma_Q$. From that time on, an annular region in which all cells are quiescent will grow. We suppose that B_0 does satisfy this requirement. We denote by $\rho_Q(t)$ the inner radius of the quiescence region. Clearly, $\rho_Q(t_Q)=B(t_Q)$ and, for $t>t_Q$,

$$\sigma(\rho_Q(t), t) = \sigma_Q\,. \tag{20}$$

We note that, for $t\in(t_Q, t_R)$, $\rho_Q(t)$ is decreasing (as a consequence of the lowering of the profile of σ) with a slope that for $t\to t_Q^+$ tends to $-\infty$. In fact, let us consider $\sigma(\rho_Q(t),t)$ as a function of time. This function is constant and equal to σ_Q so that, differentiating Eq. (20), we have

$$0 = \left.\frac{\partial\sigma}{\partial r}\right|_{\rho_Q(t)} \frac{d\rho_Q}{dt} + \left.\frac{\partial\sigma}{\partial t}\right|_{\rho_Q(t)}.$$

Since $\partial\sigma/\partial t = (\partial\sigma/\partial B)\dot{B}$ is negative and finite (see (15)), and $\sigma_r(\rho_Q(t),t) < 0$ for $t > t_Q^+$, we have $\dot{\rho}_Q(t) < 0$. In addition $\lim_{t\to t_Q^+}\dot{\rho}_Q(t) = -\infty$ because $\sigma_r(\rho_Q(t_Q), t_Q) = 0$.

At the time $t=t_R$, the cells at $r=B(t_R)=B_N$ enter the pre-necrotic status. We recall that the pre-necrotic cells do not consume oxygen (assumption *(vi)*). Hence, the boundary $\rho_R(t)$ between the quiescent region and the pre-necrotic region, and the function $\sigma(r,t)$ for $r\in[r_0,\rho_R(t)]$, are now defined by Eqs. (2), (5), and

$$\sigma(\rho_R(t), t) = \sigma_N \tag{21}$$

$$\sigma_r(\rho_R(t),t)=0\,. \tag{22}$$

Thus, $\rho_R(t)$ remains equal to $B(t_R)$ for $t\geq t_R$ (this constant value will be denoted from now on as $\bar\rho_R$), with $\sigma=\sigma_N$ in $[\bar\rho_R,B(t)]$. Because the profile of σ does not change with t for $t\geq t_R$, also the boundary ρ_Q will remain constant in time at the value $\bar\rho_Q=\rho_Q(t_R)$. Since $\chi=0$ in $Q\cup R$ we have there $\mathrm{div}\,u=0$, hence the boundary $B(t)$ satisfies

$$B\dot B=\bar\rho_Q u(\bar\rho_Q)\,,\qquad t_R<t<t_R+\tau$$

$$B(t_R)=\bar\rho_R\,.$$

After a time interval τ spent in the pre-necrotic region, cells will die and a necrotic region will originate. A necrotic region will thus exist for times larger than $t_R+\tau$. Let us consider the trajectory $r=\eta(t;t_0)$ of a cell entering the pre-necrotic region at time t_0 $(t\geq t_0\geq t_R)$; this trajectory is defined by

$$\dot\eta=u(\eta,t)\,,\qquad t_0<t<t_0+\tau \tag{23}$$

$$\eta(t_0;t_0)=\bar\rho_R\,. \tag{24}$$

As long as a cell is in the pre-necrotic region, its velocity u will be given by

$$ru(r,t)=K \tag{25}$$

with

$$K=\int_{r_0}^{\bar\rho_Q} r\chi(\sigma(r,t))\,dr\,, \tag{26}$$

K being independent of time, thus from Eqs. (23)-(26) we obtain

$$\eta^2(t;t_0)=\bar\rho_R^2+2K(t-t_0)\,.$$

At the time $t=t_0+\tau$, at which cell death occurs, the position of the cell will thus be the same irrespective of t_0. Denoting by $\bar\rho_N$ the radius that marks the interface between the pre-necrotic and the necrotic region, we have

$$\bar\rho_N=[\bar\rho_R^2+2K\tau]^{1/2}\,. \tag{27}$$

After the time $t=t_R+\tau$, recalling Eq. (1), $B(t)$ will evolve according to

$$B\dot B=K-\frac{\mu}{2}(B^2(t)-\bar\rho_N^2)$$

$$B(t_R+\tau)=\bar\rho_N\,,$$

and it will become the outer boundary of the necrotic region generated by the cord. Therefore

$$B(t)=\Big[\bar\rho_N^2+\frac{2K}{\mu}(1-\mathrm{e}^{\mu(t_R+\tau-t)})\Big]^{1/2}\,,$$

and, as $t\to\infty$, $B(t)$ will tend to the steady-state value given by

$$\bar B=\Big[\bar\rho_N^2+\frac{2K}{\mu}\Big]^{1/2}\,. \tag{28}$$

Figure 2 shows an example of the time evolution of the boundaries that characterize the tumour cord, with the successive formation around the proliferating cells of the quiescent, prenecrotic and necrotic regions.

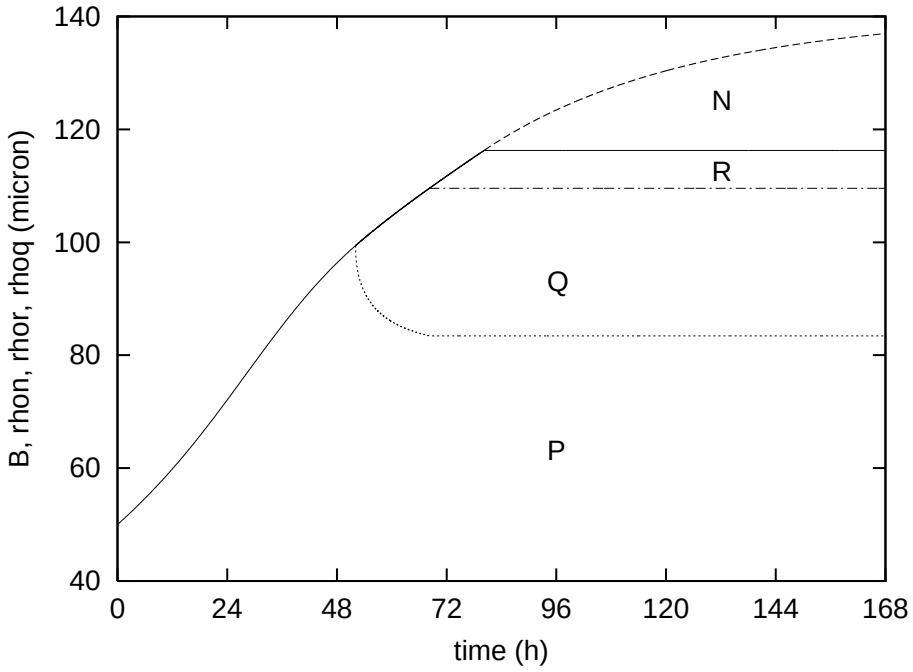

Fig. 2. Evolution of the cord boundaries. The solid line indicates the evolution of the boundary $B(t)$ until $t=t_N$ and then the interface with the necrotic region: the boundary $B(t)$ continues as the dashed line; $\rho_Q(t)$, dotted lined; $\rho_R(t)$ dash-dotted line. The regions P, Q, R and N are also indicated. Parameter values (O_2 concentration in mmHg, length in μm, time in h): $r_0=20$, $\sigma^\star=35$, $\sigma_P=20$, $\sigma_Q=2$, $\sigma_N=1$, $\mu=0.02$, $\tau=12$. Moreover: $F=0.0128$, $K=4.32$ (Casciari *et al.*, 1992); $\chi(\sigma)$ increasing as a Michaelis-Menten curve in (σ_Q,σ_P) from 0 to $\chi_0=\ln 2/T_{d0}$, with T_{d0} (doubling time of the cell population in the vicinity of the blood vessel) equal to 20.

3. Decrease of oxygen concentration in blood

Let us consider a tumour cord at the stationary state, as described in the previous section. The oxygen concentration profile and the radius $\bar\rho_R$ are solutions of Eqs. (2), (5), (21) and (22). This solution also determines the radius $\bar\rho_Q$. Let us suppose that at $t=0$ the oxygen concentration in blood drops instantaneously to a value $\sigma_1^\star<\sigma^\star$, with $\sigma_1^\star>\sigma_Q$. The profile of σ and the radius ρ_R will instantaneously follow this change, and will be given by the equations listed above with $\sigma^\star$ changed to $\sigma_1^\star$ in (5). Thereafter, σ and ρ_R will be independent of t. We will denote with the subscript $''1''$ all the quantities in the new state defined by the oxygen blood concentration $\sigma_1^\star$, thus we will have $\sigma_1(r)<\sigma(r)$ and $\bar\rho_{R1}<\bar\rho_R$. The new oxygen profile defines the new boundary $\bar\rho_{Q1}$ with the quiescent region.

Not so trivial is the description of the evolution of the boundary ρ_N for $t>0$. We note preliminarly that the pre-necrotic region at $t=0^+$ is the old pre-necrotic region augmented by the interval $[\bar\rho_{R1},\bar\rho_R)$. For $t>0$, the velocity field in the pre-necrotic region is independent of t and is given by

$$ru(r,t)=K_1 \tag{29}$$

with

$$K_1=\int_{r_0}^{\bar\rho_{Q1}} r\chi(\sigma_1(r,t))\,dr\,, \tag{30}$$

K_1 being smaller than K. Let $\rho_{N1}(t)$ denote the interface with necrosis at time t, and let us first consider the cells that were initially in the old pre-necrotic region, that is in the interval $[\bar{\rho}_R, \bar{\rho}_N]$. If at time $t \in (0, \tau]$ one of these cells has the radial position r, it is easy to see from (29)-(30) that the following relation holds

$$r^2 - \zeta^2(r,t) = 2K_1 t\,,$$

where $\zeta(r,t)$ is the radial coordinate at $t=0$ of the trajectory passing through (r,t). $\zeta(r,t)$ is given by

$$\zeta^2(r,t) - \bar{\rho}_R^2 = 2K a_0(\zeta(r,t))\,, \tag{31}$$

where $a_0(\zeta(r,t))$ is the age in the pre-necrotic region of a cell occupying the position $\zeta(r,t)$ at $t=0$. Equation (31) carries the information of the state of the system prior to the oxygen decrease. Because cell death occurs after the cell has spent the time τ in the pre-necrotic region, $\rho_{N1}(t)$ satisfies the equation

$$\rho_{N1}^2(t) - \zeta^2(\rho_{N1}(t), t) = 2K_1 t\,, \tag{32}$$

with ζ such that $a_0(\zeta)+t=\tau$. Taking into account Eq. (31), we have

$$\zeta^2(\rho_{N1}(t), t) = \bar{\rho}_R^2 + 2K(\tau - t)\,, \tag{33}$$

and thus, from Eqs. (32), (33) and in view of (27), we get

$$\rho_{N1}(t) = [\bar{\rho}_N^2 - 2(K - K_1)t]^{1/2}\,, \quad 0 < t < \tau\,. \tag{34}$$

At $t=\tau$, all the cells that initially were in the region $[\bar{\rho}_{R1}, \bar{\rho}_R)$, and that therefore entered the pre-necrotic region with age zero at $t=0$, simultaneously will die, so that the interface with the necrotic region will suddenly move inwards to the radius

$$\bar{\rho}_{N1} = [\bar{\rho}_{R1}^2 + 2K_1\tau]^{1/2}\,. \tag{35}$$

Considering the trajectories starting from $r=\bar{\rho}_{R1}$ at times larger than zero, it is easy to see that $\rho_{N1}(t)$ remains constant at the value $\bar{\rho}_{N1}$ for $t>\tau$.

In the necrotic region, according to Eq. (1), the velocity field is given by

$$ru(r,t) = K_1 - \frac{\mu}{2}(r^2 - \rho_{N1}^2(t))\,,$$

so that the evolution of the boundary B_1 will be described by

$$B_1\dot{B}_1 = K_1 - \frac{\mu}{2}(B_1^2(t) - \rho_{N1}^2(t)) \tag{36}$$

with the initial condition

$$B_1(0) = \bar{B}\,. \tag{37}$$

Integrating (36)-(37) and taking into account Eq. (34), we obtain for $0 \le t \le \tau$

$$B_1^2(t) = \bar{B}^2 \mathrm{e}^{-\mu t} - 2(K - K_1)t + (\bar{\rho}_N^2 + \frac{2K}{\mu})(1 - \mathrm{e}^{-\mu t})\,.$$

For $t>\tau$, when $\rho_{N1}(t)=\bar{\rho}_{N1}$ as given by (35), we have

$$B_1^2(t) = B_1^2(\tau)\mathrm{e}^{-\mu(t-\tau)} + (\bar{\rho}_{N1}^2 + \frac{2K_1}{\mu})(1 - \mathrm{e}^{-\mu(t-\tau)})\,.$$

Thus, for $t \to \infty$, the boundary B_1 will tend to the new stationary value given by

$$\bar{B}_1 = \big[\bar{\rho}_{N1}^2 + \frac{2K_1}{\mu}\big]^{1/2}\,. \tag{38}$$

Figure 3 shows an example of the response of the tumour cord to a decrease of the oxygen concentration in blood.

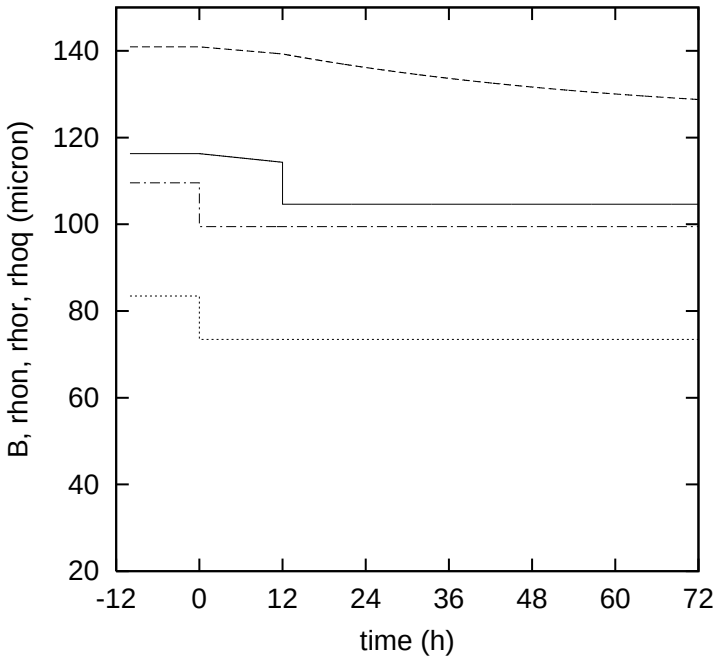

Fig. 3. Shrinkage of the tumour cord following the decrease of oxygen concentration in blood from $\sigma^\star = 35$ to $\sigma_1^\star = 25$ at $t = 0$. $B(t)$, dashed line; $\rho_N(t)$, solid line; $\rho_R(t)$, dash-dotted line; $\rho_Q(t)$, dotted line. Other cord parameters as in Fig. 2.

4. Increase of oxygen concentration in blood

Let us suppose now that at $t = 0$ the oxygen concentration in blood rises instantaneously to a value $\sigma_2^\star > \sigma^\star$. We will denote with the subscript "2" all the quantities in the new state defined by the oxygen blood concentration $\sigma_2^\star$. The profile of σ will instantaneously follow this change, and two cases can occur at $t = 0^+$: either (case I) the equations (2), (5) (with $\sigma^\star$ changed to $\sigma_2^\star$), (21) and (22) have a solution with $\rho_{R2} \leq \bar{\rho}_N$, or (case II) there exists a solution of Eqs. (2), (5) and

$$\sigma_{2r}(\bar{\rho}_N) = 0\,, \tag{39}$$

with $\sigma_2(\bar{\rho}_N) > \sigma_N$. Thus, the cells that were in the region between $\bar{\rho}_R$ and ρ_{R2} (or $\bar{\rho}_N$) leave the pre-necrotic state instantly resuming viability.

In case I, for $t > 0$, σ and ρ_R will be independent of t, with $\rho_R(t) = \bar{\rho}_{R2}$ and $\sigma(r,t) = \sigma_2(r)$, and the new oxygen profile will define the new boundary $\bar{\rho}_{Q2}$ with the quiescent region. Since $\bar{\rho}_{Q2} > \bar{\rho}_Q$, there is an instantaneous recruitment of quiescent cells into proliferation. Let $\rho_{N2}(t)$ denote the interface with necrosis at time t. The velocity field is also independent of t and, for r in $[\bar{\rho}_{R2}, \rho_{N2}(t)]$, is given by

$$ru(r,t) = K_2$$

with

$$K_2 = \int_{r_0}^{\bar{\rho}_{Q2}} r\chi(\sigma_2(r,t))\,dr\,, \tag{40}$$

K_2 being larger than K. Let us suppose $\bar{\rho}_{R2} < \bar{\rho}_N$. By considering the trajectories of the cells that were initially in the interval $[\bar{\rho}_{R2}, \bar{\rho}_N]$, and by following the derivation given in the previous

section, we obtain

$$\rho_{N2}(t) = [\bar{\rho}_N^2 + 2(K_2 - K)t]^{1/2}\,, \quad 0 < t < \tilde{t}\,,$$

where $\tilde{t}$ is the time at which the cells that were in $r = \bar{\rho}_{R2}^+$ at $t = 0$ will die, that is

$$\tilde{t} = \tau - \frac{\bar{\rho}_{R2}^2 - \bar{\rho}_R^2}{2K}\,. \tag{41}$$

For $\tilde{t} \le t \le \tau$, the interface with the necrotic region will be given by the trajectory starting from $r = \bar{\rho}_{R2}$ at time zero:

$$\rho_{N2}(t) = [\bar{\rho}_{R2}^2 + 2K_2 t]^{1/2}\,, \tag{42}$$

since the cells in $r = \bar{\rho}_{R2}^-$ at $t = 0$ resume instantly the quiescent status, and cross $\bar{\rho}_{R2}$ immediately after. For $t \ge \tau$, since ρ_{R2} is constant, ρ_{N2} is also constant and equal to

$$\bar{\rho}_{N2} = [\bar{\rho}_{R2}^2 + 2K_2\tau]^{1/2}\,. \tag{43}$$

In the case in which $\bar{\rho}_{R2} = \bar{\rho}_N$, $\tilde{t}$ will be equal to zero, and Eqs. (42) and (43) will describe the entire evolution of $\rho_{N2}(t)$.

In the necrotic region the velocity field is given by

$$ru(r,t) = K_2 - \frac{\mu}{2}(r^2 - \rho_{N2}^2(t))\,,$$

so that the evolution of the boundary B_2 will be described by

$$B_2\dot{B}_2 = K_2 - \frac{\mu}{2}(B_2^2(t) - \rho_{N2}^2(t))$$

with the initial condition

$$B_2(0) = \bar{B}\,.$$

For $t \to \infty$, the boundary B_2 will tend to the stationary value given by

$$\bar{B}_2 = \left[\bar{\rho}_{N2}^2 + \frac{2K_2}{\mu}\right]^{1/2}. \tag{44}$$

In case II, the whole cord up to $\bar{\rho}_N$ turns back to be viable, and a new phase of growth starts. This growth may be described as in section 2, with $\rho_{N2}(t)$ becoming a material interface and playing now the role of $B(t)$. Also in this case a new stationary value $\bar{\rho}_{N2}$ will be reached, and the new boundary B will tend to the stationary value given by Eq. (44), provided that K_2 be assigned the proper value according to Eq. (40).

5. Effect of the non-instantaneous recruitment from quiescence

Some experimental observations have suggested that quiescent cells reenter the proliferative cycle with a certain delay after that a recruitment stimulus has been provided to the population [15,16]. A representation of this phenomenon appears to be complex, and its accurate description would require a rather detailed cell population model. We attempted to account for this delay in our model, which is formulated in terms of the volume fraction occupied by the cells, by simplifying the dependence of cell proliferation on oxygen concentration with respect to that assumed in the previous sections. The assumption *(v)* of section 2 will thus be modified as follows.

For a viable cell in the tumour cord, as far as the proliferative activity is concerned, we will distinguish three possible states: full proliferation, quiescence or pre-necrosis, and recovery of proliferation. The proliferation rate of a fully proliferating cell is $\chi = \chi_0$, irrespective of the oxygen concentration if $\sigma > \sigma_Q$, whereas the proliferation rate of quiescent or pre-necrotic cells is zero. When σ decreases to σ_Q, both fully proliferating cells and cells in the recovery state become instantaneously quiescent. If σ increases over σ_Q at a given time, a quiescent or pre-necrotic cell passes into the recovery state and its proliferation rate is assumed to change in time in a way that depends on the age from the entrance into the quiescent state, a_Q, the cell had at the transition time. More precisely:

$$\bar{\chi}(a_Q,\theta) = \begin{cases} 0 & 0 \le \theta \le t_1(a_Q) \\ \chi_0 \dfrac{\theta - t_1(a_Q)}{t_2(a_Q) - t_1(a_Q)} & t_1(a_Q) < \theta \le t_2(a_Q)\,, \end{cases} \tag{45}$$

where θ is the time passed since the transition into the recovery state. That is, the recovery is a *transient* state in which after a delay of length t_1, χ increases linearly in time and recovers its maximum value χ_0 at a time t_2 when the cell passes to the state of full proliferation. Both the delay time t_1 and the overall duration t_2 of the recovery state are assumed to be functions of a_Q. The dependence of t_1 and t_2 on the time spent out of the cycle is suggested by the possible degradation in such a state of some proteins necessary for progressing through the cell cycle. For simplicity, we have assumed

$$t_1 = \begin{cases} c_1 a_Q & 0 \le a_Q < a_Q^\star \\ t_1^\star & a_Q \ge a_Q^\star \end{cases} \tag{46}$$

$$t_2 = \begin{cases} c_2 a_Q & 0 \le a_Q < a_Q^\star \\ t_2^\star & a_Q \ge a_Q^\star\,, \end{cases} \tag{47}$$

where $c_1 = t_1^\star / a_Q^\star$ and $c_2 = t_2^\star / a_Q^\star$, with $t_2^\star > t_1^\star$.

It is easy to see that the above hypotheses do not change the behaviour of the cord with respect to that illustrated in section 3, when the oxygen concentration in blood suddenly decreases. On the contrary, in the case of the increase of oxygen concentration in blood, the cord response will be different as described in the following.

As in section 4, let us assume that at $t = 0$ the oxygen concentration in blood rises instantaneously to a value $\sigma_2^\star$, and first assume that case I occurs. Thus, for $t > 0$, σ, ρ_R and ρ_Q will be independent of t with $\rho_{R2}(t) = \bar{\rho}_{R2}$, $\bar{\rho}_R < \bar{\rho}_{R2} \le \bar{\rho}_N$, and $\rho_{Q2}(t) = \bar{\rho}_{Q2} > \bar{\rho}_Q$. The cells in the region $[\bar{\rho}_Q, \bar{\rho}_{Q2}]$ will pass at $t = 0$ from the quiescent (or pre-necrotic) state to the recovery state.

Let $r=\hat{\eta}(t)$ be the trajectory of the cells initially in $\bar{\rho}_Q$. Since for $r<\hat{\eta}(t)$, according to our present assumptions, it is $\operatorname{div} u=\chi_0$, we have

$$\hat{\eta}(t)=[r_0^2+(\bar{\rho}_Q^2-r_0^2)\mathrm{e}^{\chi_0 t}]^{1/2}\,. \tag{48}$$

We denote by $\hat{t}$ the time at which $\hat{\eta}(t)$ reaches $r=\bar{\rho}_{Q2}$. For $\hat{\eta}(t)\le r\le\bar{\rho}_{Q2}$, $0\le t\le\hat{t}$, let us define the function $a_Q(r,t)$ as the age a_Q possessed at $t=0$ by the cells that at time t are at the position r. In the same set, let $\tilde{\chi}(r,t)$ denote the proliferation rate at the position r and time t. In view of (45), we have

$$\tilde{\chi}(r,t)=\begin{cases}\bar{\chi}(a_Q(r,t),t) & 0\le t<t_2(a_Q(r,t))\\ \chi_0 & t\ge t_2(a_Q(r,t))\,.\end{cases} \tag{49}$$

Thus $u(r,t)$ satisfies the equation

$$\operatorname{div} u=\tilde{\chi}(r,t) \tag{50}$$

with the boundary condition

$$\hat{\eta}(t)u(\hat{\eta}(t),t)=\frac{\chi_0}{2}(\hat{\eta}^2(t)-r_0^2)\,. \tag{51}$$

Taking into account that for $t\le 0$ it is $\operatorname{div} u=0$ in the interval $[\bar{\rho}_Q,\bar{\rho}_{Q2}]$, we obtain

$$a_Q(r,t)=\frac{\zeta^2(r,t)-\bar{\rho}_Q^2}{\chi_0(\bar{\rho}_Q^2-r_0^2)}\,, \tag{52}$$

where $\zeta(r,t)$ is the initial position of the cells that are at the radial position r at time t. $\zeta(r,t)$ is such that

$$\eta(t;\zeta(r,t))=r\,, \tag{53}$$

where η is the solution of

$$\dot{\eta}=u(\eta,t) \tag{54}$$

$$\eta(0;\zeta(r,t))=\zeta(r,t)\,. \tag{55}$$

The problem that arises is to find the functions $u(r,t)$ and $\zeta(r,t)$ that satisfy Eqs. (49)-(55).

Let us look at a cell initially at $r=\hat{r}\in[\bar{\rho}_Q,\bar{\rho}_{Q2}]$, with $\hat{r}$ less than a suitable value. As t increases, after the time $c_1a_Q(\hat{r},0)$ the proliferative activity will start and after the time $c_2a_Q(\hat{r},0)$ the recovery of proliferation will be complete. Thus two surfaces will arise in the cord from $r=\bar{\rho}_Q$, that mark the outer boundary of the region of full recovery and the inner boundary of the region in which the proliferation rate is still equal to zero. We denote these non-material boundaries as $\phi_P(t)$ and $\phi_Q(t)$, respectively, and these boundaries are implicitly defined by

$$c_2a_Q(\phi_P(t),t)=t$$

$$c_1a_Q(\phi_Q(t),t)=t\,.$$

It is easy to recognize that $\hat{\eta}(t)<\phi_P(t)<\phi_Q(t)$.

If $a_Q(\bar{\rho}_{Q2},0)>a_Q^\star$, there exists a radius $r^\star<\bar{\rho}_{Q2}$ such that $a_Q(r^\star,0)=a_Q^\star$. Let $r=\eta^\star(t)$ be the trajectory starting from $r^\star$ at $t=0$, and let $t^\star$ be the time at which $\eta^\star$ reaches $\bar{\rho}_{Q2}$. Four cases are possible:

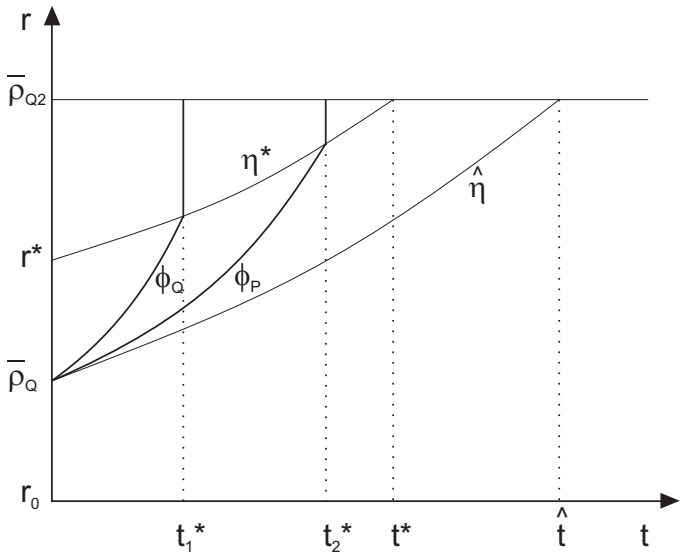

Fig. 4. Schematic representation of the characteristic boundaries of the recovery transient.

(a) $a_Q(\bar{\rho}_{Q2},0)\le a_Q^\star$;
(b) $a_Q(\bar{\rho}_{Q2},0)> a_Q^\star$, $t^\star\le t_1^\star$;
(c) $a_Q(\bar{\rho}_{Q2},0)> a_Q^\star$, $t_1^\star< t^\star\le t_2^\star$;
(d) $a_Q(\bar{\rho}_{Q2},0)> a_Q^\star$, $t^\star> t_2^\star$.

In cases (a) and (b), both $\phi_Q(t)$ and $\phi_P(t)$ will reach $r=\bar{\rho}_{Q2}$ at the times $\bar{t}_1$ and $\bar{t}_2$ that are, respectively, not greater than $t_1^\star$ and less than $t_2^\star$. In case (c), $\phi_Q(t)$ crosses the trajectory $\eta^\star$ at $t=t_1^\star$, whereas $\phi_P(t)$ will reach $r=\bar{\rho}_{Q2}$ at $\bar{t}_2< t_2^\star$. At the time $t_1^\star$ all the cells between $\eta^\star(t_1^\star)$ and $\bar{\rho}_{Q2}$ will simultaneously start the recovery of proliferation. In case (d), $\phi_P(t)$ crosses the trajectory $\eta^\star$ at $t=t_2^\star$, and the cells between $\eta^\star(t_2^\star)$ and $\bar{\rho}_{Q2}$ will simultaneously achieve $\chi=\chi_0$ (see Fig. 4). Let us denote by t_{max} the time at which the recovery of proliferation is complete: t_{max} will be equal to $\bar{t}_2$ in cases (a), (b), (c) and to $t_2^\star$ in case (d), and in all cases $t_{max}<\hat{t}$. Thus the full proliferation is achieved before the region $r\in[\bar{\rho}_Q,\bar{\rho}_{Q2}]$ is replenished by the cells coming from the old proliferating region $(r_0,\bar{\rho}_Q)$.

In order to describe the evolution of the interface with the necrotic region, $\rho_{N2}(t)$, we observe that the velocity field for $r\in[\bar{\rho}_{Q2},\rho_{N2}(t)]$ can be expressed as

$$ru(r,t)=K_2(t)\,,$$

where, for $t\le t_{max}$, $K_2(t)$ is increasing and given by

$$K_2(t)=\frac{\chi_0}{2}(\hat{\eta}^2(t)-r_0^2)+\int_{\hat{\eta}(t)}^{\bar{\rho}_{Q2}} r\tilde{\chi}(r,t)\,dr\,, \tag{56}$$

whereas, for $t>t_{max}$, $K_2(t)$ will be constant and equal to

$$K_2=\frac{\chi_0}{2}(\bar{\rho}_{Q2}^2-r_0^2)\,.$$

Proceeding therefore as in section 4, for $0<t<\tilde{t}$, $\tilde{t}$ being given by Eq. (41), we have

$$\rho_{N2}(t)=\left[\bar{\rho}_N^2+2\int_0^t(K_2(s)-K)\,ds\right]^{1/2}, \tag{57}$$

with $K=(\chi_0/2)(\bar{\rho}_Q^2-r_0^2)$ according to (26). For $\tilde{t}\le t\le\tau$ the interface with the necrotic region will become a material boundary and is given by

$$\rho_{N2}(t)=\left[\bar{\rho}_{R2}^2+2\int_0^t K_2(s)\,ds\right]^{1/2}. \tag{58}$$

For $t>\tau$, the interface turns back to be non-material and increases until $t=t_{max}+\tau$ according to

$$\rho_{N2}(t)=\left[\bar{\rho}_{R2}^2+2\int_{t-\tau}^t K_2(s)\,ds\right]^{1/2}, \tag{59}$$

and then remains constant and equal to

$$\bar{\rho}_{N2}=[\bar{\rho}_{R2}^2+2K_2\tau]^{1/2}, \tag{60}$$

with K_2 given by (56). In the case in which $\bar{\rho}_{R2}=\bar{\rho}_N$, $\tilde{t}$ will be equal to zero and Eqs. (58)-(60) will describe completely the evolution of $\rho_{N2}(t)$.

In case II, as recognized in the previous section, the whole cord up to $\bar{\rho}_N$ turns back to be viable at $t=0^+$, and a new phase of growth starts. In describing this growth, the recovery transient has to be accounted for, since the cells in a region that can extend up to $\bar{\rho}_N$ will pass to the recovery state. The recovery phase can be described as above, taking into account that the boundary ρ_{Q2} will change in time, until the time at which it is $\sigma(\rho_{N2}(t),t)=\sigma_N$ (see section 2). We will not give here, however, further details about this case, whose study can be carried on by the treatment of section 2 suitably modified.

The existence of the solution of the problem defined by Eqs. (49)-(55) (and therefore the existence of the boundaries ϕ_P and ϕ_Q) was assessed in [17] by means of a constructive method. Since the proof is very long and technical, it will not be reported here. The numerical solution of Eqs. (49)-(55) has been obtained by means of an iterative approximating procedure proposed in [17] and is briefly described as follows with reference, for simplicity, to case I.

Let us denote by Ω the set of (r,t) points such that $\hat{\eta}(t)\le r\le\bar{\rho}_{Q2}$, $0\le t\le\hat{t}$, with $\hat{\eta}(t)$ given by Eq. (48), and let $\hat{r}_i$, $i=1,\cdots,n+1$, be equispaced grid points in the interval $[\bar{\rho}_Q,\bar{\rho}_{Q2}]$. Let $\tilde{\chi}^k(r,t)$ be the k-th approximation of $\tilde{\chi}(r,t)$ on Ω. By means of Eqs. (50)-(51), the velocity field $u^k(r,t)$ is defined and the trajectories $\eta_i^k(t)$ starting from $\hat{r}_i$ can be computed from Eq. (54). Thus, $\tilde{\chi}(\eta_i^k(t),t)$ is computed by using Eqs. (49) and (52), in which it is $\zeta(\eta_i^k(t),t)=\hat{r}_i$. By linear interpolation on the above values of $\tilde{\chi}$ computed over the trajectories, the new approximation $\tilde{\chi}^{k+1}(r,t)$ is obtained. Note that, by determining the times t_{1i} and t_{2i} on each trajectory through Eqs. (46) and (47), the values of the $k+1$-th approximations of ϕ_P and ϕ_Q at these times are also determined as $\phi_Q^{k+1}(t_{1i})=\eta_i^k(t_{1i})$ and $\phi_P^{k+1}(t_{2i})=\eta_i^k(t_{2i})$. Starting with $\tilde{\chi}^1(r,t)=0$ on Ω, with meaningful values of the parameters, the procedure achieved a reasonable convergence in 4-6 steps.

Figure 5 compares the increase of cord radius, as a consequence of an increase of oxygen concentration in blood, computed in the case of instantaneous recovery from quiescence to the case of delayed recovery. Because of the marked increment in $\sigma^\star$ (from 35 to 70 mmHg), case II occurs. To enhance the effect of the delay, a small value of $a_Q^\star=2$ h, with $t_1^\star=t_2^\star=14$ h have been chosen. We recall that in the istantaneous case the boundary between full proliferation and of zero proliferation coincides with the boundary $\rho_{Q2}(t)$, whereas in this simulation of the delayed case this boundary is given by $\phi_P(t)$ up to $t_1^\star=t_2^\star$. In the delayed case, the stationary state is substantially reached after a delay of about 4 h.

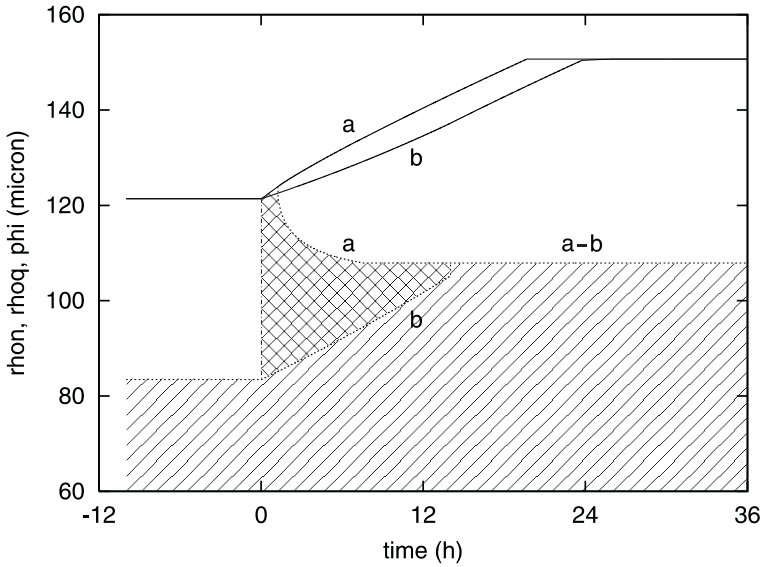

Fig. 5. Expansion of the tumour cord following the increase of oxygen concentration in blood from $\sigma^\star = 35$ to $\sigma_2^\star = 70$ at $t = 0$. Instantaneous (a) and delayed (b) recruitment of quiescent and pre-necrotic cells: $\rho_N(t)$, solid lines; boundary between $\chi = \chi_0$ and $\chi = 0$, dotted lines; $a_Q^\star = 2\,\mathrm{h}$ and $t_1^\star = t_2^\star = 14\,\mathrm{h}$. Cord parameters as in Fig. 2 except: $\chi(\sigma)$ equal to χ_0 (with $T_{d0} = 20$) for $\sigma \geq \sigma_Q$ and zero otherwise. The hatched area represents the region of full proliferation; the cross-hatched area indicates the region where $\chi = 0$ during the delayed recovery.

6. Comparison wth experimental data and concluding remarks

Hirst *et al.*, 1991 [13] measured the changes in the radius of tumour cords of RH carcinoma implanted in mice when the animals were breathing air with 10% O_2 and 100% O_2. These data are replotted in Fig. 6 and show a decrement and, respectively, an increment of cord radius, with some lag before the new stationary value is reached. A reasonable fitting of the data (including the cord radius of the control) has been obtained by choosing the model parameters as indicated in the legend of Fig. 6, and changing $\sigma^\star$ from 57.5 to 39 mmHg and, respectively to 71 mmHg. The value of T_{d0} has been taken according to the cell cycle time reported in [18] for the same tumour. No meaningful differences were found by simulating the increase of cord radius when either the delayed recovery from quiescence or the instantaneous recovery was assumed. It might be surprising that the effect of a five-fold increase in oxygen breathed by the animal be matched in the model by an increase of $\sigma^\star$ of only 23.5%, whereas halving the breathed oxygen leads to a decrease of $\sigma^\star$ of 32.2%. This fact can be explained by considering that oxygen in blood is mainly transported as bound to hemoglobin, and that hemoglobin is almost saturated in the normal breathing conditions (see the saturation curves reported in [19]). It has to be noted that the available data do not accurately describe the transient phase of the change of cord radius, which is actually predicted by the model, so that the value of the parameter τ remains rather uncertain.

In conclusion, we may observe that the proposed model appears able to describe the changes in tumour cord morphology induced by changes of oxygen concentration in blood. The inclusion in the model of a delayed exit from quiescence does not seem to modify significantly the dynamics of the expansion of the cord when oxygen in blood is increased, unless rather extreme situations occur. However, the description of this phenomenon might be of importance in other cases,

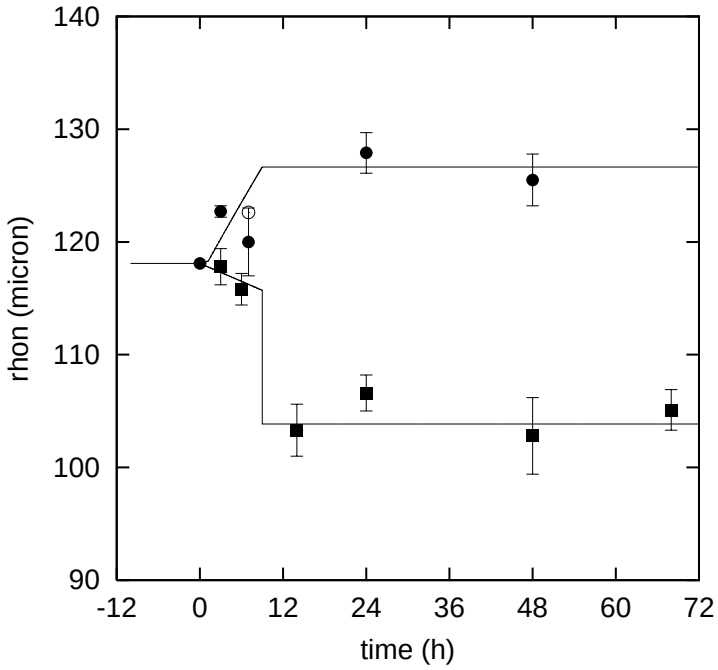

Fig. 6. Experimental data of cord radius after exposure to oxygen tensions lower (squares) or higher (circles) than normal (replotted from Hirst *et al.*, 1991 [13]; the open circle represents the point at 6 h corrected by excluding an outlier, see [13]). Curves of $\rho_N(t)$ as predicted by the model (solid lines) according to the theory of sections 3 and 4. Parameter values as in Fig. 2 except: $r_0 = 10$, $\sigma^\star = 57.5$, $\chi(\sigma)$ equal to χ_0 (with $T_{d0} = 21.5$) for $\sigma \geq \sigma_Q$ and zero otherwise, $\tau = 9$. Moreover: $\sigma_1^\star = 39$ (oxygen decrease), $\sigma_2^\star = 71$ (oxygen increase).

such as the reoxygenation of tumour cells during a therapeutic schedule, to predict the effects of repeated doses. On the other hand, the description of cord formation is highly idealized since we assumed a vasculature of identical, parallel and equispaced vessels leading to the formation of identical cords, that is not in accordance with the experimental observations showing a large variability of cord radius inside the same tumour [13]. Moreover, it is known that tumour vascularization is an evolving process driven by angiogenesis, although in the core region of the tumour this process could be less active. In spite of these limitations, our description of the appearance in a finite time of isolated tumour cords due to the formation of surrounding necrosis could be a general feature which is maintained in a much more heterogeneous system.

References

1. I.F. Tannock (1968) The relation between cell proliferation and the vascular system in a transplanted mouse mammary tumour. *Br. J. Cancer* **22**, 258-273.

2. D.G. Hirst and J. Denekamp (1979) Tumour cell proliferation in relation to the vasculature. *Cell Tissue Kinet.* **12**, 31-42.

3. J.V. Moore, H.A. Hopkins and W.B. Looney (1984) Tumour-cord parameters in two rat hepatomas that differ in their radiobiological oxygenation status. *Radiat. Environ. Biophys.* **23**, 213-222.

4. J.V. Moore, P.S. Hasleton and C.H. Buckley (1985) Tumour cords in 52 human bronchial and cervical squamous cell carcinomas: Inferences for their cellular kinetics and radiobiology. *Br. J. Cancer* **51**, 407-413.

5. A. Bertuzzi and A. Gandolfi (2000) Cell kinetics in a tumour cord. *J. theor. Biol.* **204**, 587-599.

6. A. Bertuzzi, A. Fasano, A. Gandolfi and D. Marangi (2002) Cell kinetics in tumour cords studied by a model with variable cell cycle length. *Math. Biosci.* **177&178**, 103-125.

7. G.F. Webb (2002) The steady state of a tumor cord cell population. *J. Evolut. Equat.* **2**, 425-438.

8. J. Dyson, R. Villella-Bressan and G. Webb, The steady state of a maturity structured tumor cord cell population. *Discrete Contin. Dynam. Systems B*, in press.

9. M.I.G. Bloor and M.J. Wilson (1999) The non-uniform spatial development of a micrometastasis. *J. Theor. Med.* **2**, 55-71.

10. A. Bertuzzi, A. Fasano and A. Gandolfi (2000) A mathematical model for the growth of tumor cords incorporating the dynamics of a nutrient. In *Free Boundary Problems: Theory and Applications II* (Edited by N. Kenmochi), pp. 31-46, Gakkotosho, Tokyo.

11. A. Bertuzzi, A. Fasano and A. Gandolfi, A free boundary problem with unilateral constraints describing the evolution of a tumour cord under the influence of cell killing agents, in press.

12. A. Bertuzzi, A. d'Onofrio, A. Fasano and A. Gandolfi (2003) Regression and regrowth of tumour cords following single-dose anticancer treatment. *Bull. Math. Biol.* **65**, 903-931.

13. D.G. Hirst, V.K. Hirst, B. Joiner, V. Prise and K.M. Shaffi (1991) Changes in tumour morphology with alterations in oxygen availability: further evidence for oxygen as a limiting substrate. *Br. J. Cancer* **64**, 54-58.

14. D.G. Hirst, B. Joiner and V.K. Hirst (1991) Is oxygen the limiting substrate for the expansion of cords around blood vessels in tumours? In *Oxygen Transport to Tissue XV* (Edited by P. Vaupel *et al.*), pp. 431-436, Plenum Press, New York.

15. C.A. Wallen, R. Higashikubo and L.A. Dethlefsen (1984) Murine mammary tumour cells in vitro. II. Recruitment of quiescent cells. *Cell Tissue Kinet.* **17**, 79-89.

16. J.P. Freyer and P.L. Schor (1989) Regrowth kinetics of cells from different regions of multicellular spheroids of four cell lines. *J. Cell. Physiol.* **138**, 384-392.

17. L. Filidoro (2001) *Un modello matematico per l'evoluzione delle corde tumorali*, Degree Thesis, University of Florence.

18. D.G. Hirst, J. Denekamp and B. Hobson (1982) Proliferation kinetics of endothelial cells in 3 mammary carcinomas. *Cell Tissue Kinet.* **15**, 251-261.

19. D.K. Kelleher, O. Thews and P. Vaupel (1997) Hypoxyradiotherapy: lack of experimental evidence for a preferential radioprotective effect on normal versus tumor tissue as shown by direct oxygenation measurements in experimental sarcomas. *Radiother. Oncol.* **45**, 191-197.